Microscopic Wetting Phenomena

Joseph Hautman and Michael L. Klein
Department of Chemistry, University of Pennsylvania, Philadelphia, Pennsylvania 19104-6323
(Received 14 June 1991)

Molecular-dynamics calculations have been used to investigate wetting phenomena on a microscopic length scale. The model systems consist of 90 water molecules on either hydrophobic or hydrophilic surfaces formed by monolayers of long-chain molecules with terminal $-CH_3$ or -OH groups. As in experiment, these two surfaces exhibit qualitatively different wetting behavior which is characterized by a microscopic analog of the contact angle.

PACS numbers: 68.45.Gd, 68.10.Cr, 82.65.−i

Wetting phenomena have long served as a useful means of characterizing surfaces [1–4]. Although quantities such as the contact angle are known to be sensitive to microscopic structure, much of the theory in the field has dealt with the role of long-range interactions [4]. Details of the relationship between microscopic surface structure and interfacial geometry are, for the most part, not well understood. The usual description of the wetting of a solid surface is based on Young's equation [5] which relates the contact angle θ of a liquid drop on a planar substrate to the free energies of the three interfaces involved: $\cos\theta = (\gamma_{sv} - \gamma_{sl})/\gamma_{lv}$, where γ_{ab} is the surface free energy of the a-b interface with a and b representing either the solid (s), liquid (l), or vapor (v) phase. Direct experimental verification of Young's equation is still lacking [6].

Microscopic models provide another means of examining the relationship between contact angle and surface free energies. Indeed, studies of a Lennard-Jones liquid in contact with a solid surface were inconsistent with Young's equation [7]. This discrepancy was attributed to the limited size of the simulation system. However, the accuracy of the method used to estimate the contact angle has been questioned [8]. Recent experiments have revealed systems in which the classical theories of wetting do not apply [9,10] and theoretical models have begun to incorporate the discrete nature of the phases on molecular length scales [11]. Experimental studies of wetting have benefited from recent advances in the fabrication of functionalized organic surfaces [12,13]. Wetting has been a useful probe in the development of these layers [14–17], and the composition of self-assembled layers can be controlled to create ideal substrates for studies of fundamental wetting phenomena [9,17].

In this Letter we report results from molecular-dynamics simulations of patches of water molecules in contact with both polar and nonpolar surfaces. As one might have anticipated we observe dramatic differences in the configurations adopted by the water molecules on the two surfaces. Moreover, we find a surprising quantitative correspondence between the average shape of the water cluster, characterized by a microscopic analog of the contact angle, and the geometries observed in macroscopic contact-angle measurements [14–17].

The surfaces of interest consisted of a layer of long-chain alkylthiol molecules $[SH(CH_2)_{11}X]$ on a gold substrate. These molecules self-assemble into a monolayer of thiolates with the sulfur headgroup chemisorbed to the substrate and the tailgroup ($X = CH_3$ or OH) confined to the exposed surface region. Methyl-terminated chains have been shown to chemisorb in a $\sqrt{3}\times\sqrt{3}R30°$ triangular lattice on the Au(111) surface [18]. The CH_2 chains are close packed, predominantly all-*trans*, and tilted with respect to the surface normal [14]. Models of these monolayers have been developed in earlier simulation studies and reproduce many of the observed properties [19,20]. In the present study we use a model in which the CH_2 and CH_3 groups are represented by spherical pseudoatoms [21]. The C-C bond lengths are held fixed, but the chains are otherwise flexible [22]. For the water molecules we have used one of the highly successful empirical pair potentials [23]. Water molecules interact with the chains via potentials derived from the geometrical mean of the Lennard-Jones parameters, plus electrostatic interactions. The neutral CH_3-terminated chains form a nonpolar surface while the -OH terminal group, with partial charges $-0.07e$ on the oxygen, $0.435e$ on the hydrogen, and $0.265e$ on the adjacent carbon atom [24], can form a polar surface. Chain pseudoatoms and water molecules interact with the underlying substrate through a 12-3 potential as described in Ref. [19]. The detailed headgroup-substrate interaction is highly simplified—we have ignored the ionization of the thiolate headgroup since we are predominantly interested in the outer surface of the layer.

The simulation cell contained 90 water molecules and 90 chains. The latter were arranged in the experimentally observed triangular lattice (21.4 $Å^2$ per molecule) with periodic boundary conditions in the plane of the surface. The long-ranged Coulomb interactions were handled with a version of the Ewald method [25]. To improve the efficiency of the simulation without affecting structural ensemble averages, the mass of the explicit hydrogen atoms was increased by a factor of 10.

On the CH_3-terminated surface the water molecules were initially arranged in a hydrogen-bonded patch of monolayer thickness, a configuration which was metastable at a temperature of 100 K. The velocities were scaled to 200 K and a constant-temperature molecular-dynamics run was carried out for a total of 350 ps using the Nosé

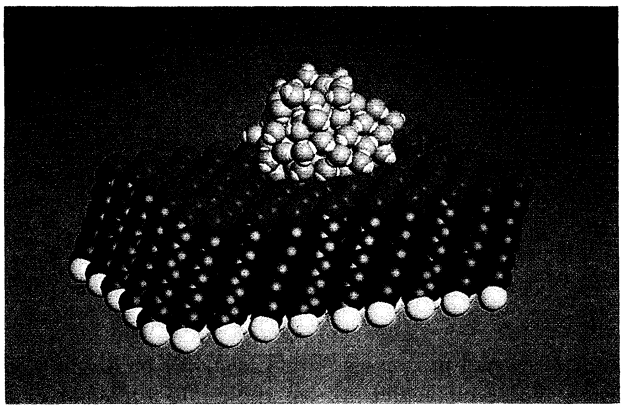

FIG. 1. Final configuration from a simulation of water molecules on a methyl-terminated monolayer. The molecules making up the layer consist of a sulfur headgroup (yellow), CH_2 pseudoatoms (blue), and a methyl tailgroup (purple). The O atom on the water molecule is orange and the H is white.

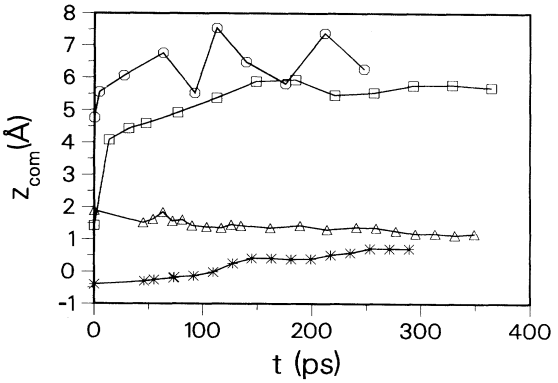

FIG. 2. Variation in the height of the center of mass of the water overlayer, $z_{c.m.}$, with time. ○, methyl surface at 300 K; □, methyl surface at 200 K; △, -OH surface at 300 K from initial "patch" configuration; ∗, -OH surface from uniform initial configuration.

method [26] with a time step of 4.5×10^{-3} ps. In the course of the simulation the water molecules gradually reorganized to form a more compact cluster. Figure 1 shows a snapshot of the system at the end of the simulation. The cluster adopts an average shape which resembles the idealized droplet geometry of a sphere intersecting a plane. The evolution of the center-of-mass position of the water molecules in the direction normal to the surface, $z_{c.m.}$, is shown in Fig. 2. Additional runs were carried out with the system held at 300 K. The fluctuations in the shape of the droplet were larger in this case, as was the mean value of $z_{c.m.}$. At this temperature occasional "evaporation" of water molecules from the cluster was observed. This is expected since the desorption temperature for water on the methyl-terminated surface, under ultrahigh vacuum, is 150 K [15]. To conserve water molecules, a reflecting barrier was placed 25 Å above the chain surface, thus imposing a microscopic vapor pressure on the system. As a test of the sensitivity of these results to initial water configuration, a second run was started with the same number of water molecules (one per chain) spread out uniformly over the surface in a triangular lattice. This system also formed a droplet at 200 K.

Simple interpretations of wetting measurements have been questioned on the basis that the "solid" surface is likely to be distorted from the planar shape of the free surface [6,27]. In the present case, the deviation from planarity around the droplet is less than 0.2 Å.

The polar surface was studied as follows: a patch of water (as above) was placed on an OH-terminated surface which had previously been equilibrated for 90 ps to allow for reconstruction of the polar groups at the outer surface [20]. This system displayed a slower dynamical evolution, limited by the formation and breaking of chain-chain, chain-water, and water-water hydrogen bonds. The final configuration is shown in Fig. 3 after 350 ps at 300 K. The water is more spread out over the surface in this case than on the hydrophobic methyl surface resulting in much lower values of $z_{c.m.}$ (Fig. 2). The height of the center of mass drifts toward lower values and does not appear to stabilize over this time scale.

Another run with the same OH-terminated system was

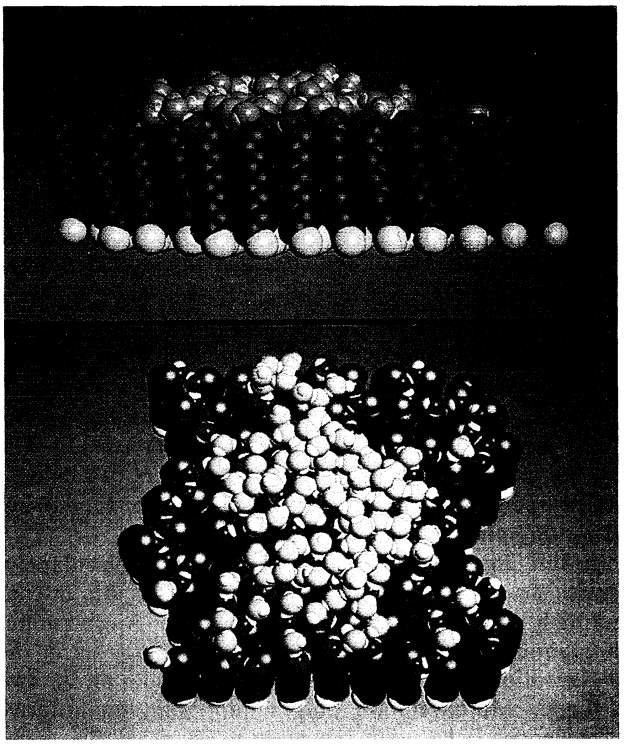

FIG. 3. Two views of the final configuration for water molecules on a monolayer with polar (-OH) tailgroups. The colors are as in Fig. 1 with the addition of O (red) and H (white) tailgroup atoms.

started with the 90 water molecules distributed uniformly in an ordered array over an unreconstructed surface [28]. In this case, $z_{c.m.}$ *increased* steadily over the course of the run (Fig. 2) apparently converging with the previous run. After 300 ps the water molecules had clustered but remained more uniformly distributed than the water started from a patch.

The results shown in Figs. 1 and 3 correlate sufficiently well with deductions based on macroscopic contact-angle measurements [13–17] that it is tempting to seek a microscopic analog. A microscopic wetting angle is calculated here by comparing the average height of the center of mass, $\langle z_{c.m.}\rangle$, of the water cluster to that of an ideal sessile drop in the shape of a sphere intersecting a surface plane. The position of the sphere relative to the plane is determined by the center-of-mass position and the condition that the volume of the sphere in the half space above the surface plane contains the correct number of water molecules (assuming a uniform density in the idealized drop equal to that of bulk water). Figure 4 shows such a construction superimposed on a single representative configuration. The angle of intersection between the surface of the sphere and the plane defines a contact angle for the droplet, which is related to $\langle z_{c.m.}\rangle$ by the formula

$$\langle z_{c.m.}\rangle = (2)^{-4/3} R_0 \left(\frac{1-\cos\theta}{2+\cos\theta}\right)^{1/3} \frac{3+\cos\theta}{2+\cos\theta}, \qquad (1)$$

where $\langle z_{c.m.}\rangle$ is measured relative to the planar surface and $R_0(3N/4\pi\rho_0)^{1/3}$, the radius of a free spherical drop of N water molecules at uniform density $\rho_0 = 0.033$ Å^{-3}. The position of the center of mass of the water molecules was calculated with respect to the surface defined by the average height of the CH_3 group plus its van der Waals radius. In the case of the OH-terminated chains the positions and radii of the O atoms were used.

The microscopic contact angles elicited in this way are $\theta = 120° \pm 10°$ for the methyl-terminated system at 200 K, and $135° \pm 15°$ at 300 K. The corresponding macroscopic advancing contact angle, at room temperature, is about 115° (104° receding) [14,17]. Although a geometric interpretation of Eq. (1) is less clear in the -OH case, there is no difficulty in applying the formalism to obtain a characterization of the wettability: The system started from a patch, averaged over the last 20 ps, gave a value $\theta = 17° \pm 2°$, while the system started with uniformly dispersed water molecules gave $\theta \approx 5°$. The seemingly nonergodic behavior on the simulated -OH surface is perhaps not surprising given the large amount of hysteresis and wide variation in contact angles measured in laboratory experiments, which are variously quoted as $< 10°$ [14,17], 25° [16], and 42° [29] for advancing drops, with smaller values generally obtained for the receding case. Scanning-tunneling-microscope (STM) measurements on the OH-terminated surface have recently been reported [29]. These images, made under a humid environment, show evidence of voids from 10 to 50 Å across and extending deep into the layer. Lateral inhomogeneity on the scale of 10–20 Å is also evident in the simulated OH-terminated systems; however, this is mostly due to the clustering of water molecules. In this relatively small and defect-free model, we do not observe voids more than few water molecules deep. Recent STM studies of methyl-terminated layers on Au suggest that the probe tip penetrates through the chains and images the sulfur headgroups [30]. A similar difficulty may be associated with imaging the surface of the OH-terminated layers.

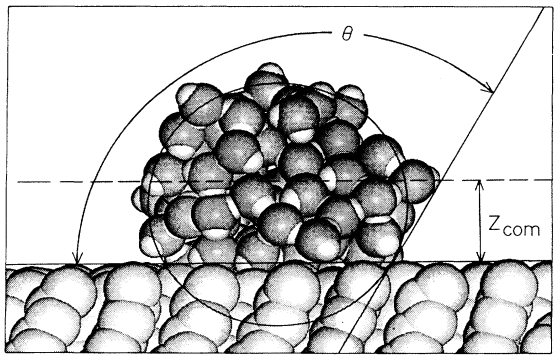

FIG. 4. Construction used to calculate a microscopic contact angle from time-averaged water configurations, superimposed on a view of the configuration shown in Fig. 1.

The extrapolation of relationships characterizing macroscopic wetting phenomena down to molecular length scales is ultimately limited by the thickness of the local water-vapor interface. Computer simulations [31] and experiment [32] on free water surfaces yield interfacial widths (≈ 3 Å) significantly less than the radius of curvature R_c for the sphere shown in Fig. 4. Moreover, the average energy per water molecule in the droplet is only 15% less than the bulk value. This is likely why the contact-angle estimate for the small droplet is so similar to that of the macroscopic drop. In the case of the OH-terminated chains the validity of the macroscopic picture is limited not by R_c, which is large, but by the thickness of the overlayer, one or two molecules in the present simulation.

In summary, simulations of relatively small numbers of water molecules on polar and nonpolar organic surfaces display properties strikingly similar to the corresponding macroscopic wetting phenomena on hydrophilic and hydrophobic surfaces. The present results suggest that simulations on the order of the 10^3 particles may be sufficient to predict macroscopic properties such as the wetting contact angle.

This research was supported by the National Institutes of Health through Grants No. GM 40712 and No. RR 04882.

[1] A. W. Adamson, *Physical Chemistry of Surfaces* (Wiley,

New York, 1982), 5th ed.
[2] J. S. Rowlinson and B. Widom, *Molecular Theory of Capillarity* (Clarendon, Oxford, 1982).
[3] P. G. de Gennes, Rev. Mod. Phys. **57**, 827 (1985).
[4] W. Zisman, in *Contact Angle, Wettability and Adhesion,* edited by F. M. Fowkes, Advances in Chemical Series Vol. 43 (American Chemical Society, Washington, DC, 1964).
[5] T. Young, Philos. Trans. Roy. Soc. (London) **95**, 65 (1805).
[6] *Physical Chemistry of Surfaces* (Ref. [1]), p. 403.
[7] G. Saville, J. Chem. Soc. Faraday Trans. II **73**, 1122 (1977).
[8] M. J. P. Nijmeijer, C. Bruin, A. F. Bakker, and J. M. J. van Leeuwen, Physica (Amsterdam) **160A**, 166 (1989).
[9] P. Silberzan and L. Léger, Phys. Rev. Lett. **66**, 185 (1991).
[10] F. Heslot, A. M. Cazabat, and P. Levinson, Phys. Rev. Lett. **62**, 1286 (1989).
[11] J. F. Joanny and P. G. de Gennes, Physica (Amsterdam) **147A**, 238 (1987).
[12] J. Sagiv, J. Am. Chem. Soc. **102**, 92 (1980).
[13] R. G. Nuzzo and D. L. Allara, J. Am. Chem. Soc. **105**, 4481 (1983).
[14] C. D. Bain, E. B. Troughton, Y-T. Tao, J. Evall, G. M. Whitesides, and R. G. Nuzzo, J. Am. Chem. Soc. **111**, 321 (1989).
[15] R. G. Nuzzo, L. H. Dubois, and D. L. Allara, J. Am. Chem. Soc. **112**, 558 (1990); L. H. Dubois, B. R. Zegarski, and R. G. Nuzzo, J. Am. Chem. Soc. **112**, 570 (1990).
[16] S. D. Evans, R. Sharma, and A. Ulman, Langmuir **7**, 156 (1991).
[17] G. M. Whitesides and P. E. Laibinis, Langmuir **6**, 87 (1990); P. E. Laibinis and G. M. Whitesides (to be published).
[18] L. S. Strong and G. M. Whitesides, Langmuir **4**, 546 (1988).
[19] J. Hautman and M. L. Klein, J. Chem. Phys. **91**, 4994 (1989); **93**, 7483 (1990).
[20] J. Hautman, J. Bareman, W. Mar, and M. L. Klein, J. Chem. Soc. Faraday Trans. **87**, 2031 (1991).
[21] J.-P. Ryckaert and A. Bellemans, J. Chem. Soc. Faraday Discuss. **66**, 95 (1978).
[22] P. van der Ploeg and H. J. C. Berendsen, J. Chem. Phys. **76**, 3271 (1982).
[23] H. J. C. Berendsen, J. P. M. Postma, W. F. van Gunsteren, and J. Hermans, in *Intermolecular Forces,* edited by B. Pullman (Reidel, Dordrecht, 1981).
[24] W. L. Jorgensen, J. Phys. Chem. **90**, 6379 (1986).
[25] J. Hautman and M. L. Klein, Mol. Phys. (to be published).
[26] S. Nosé, Mol. Phys. **52**, 255 (1984); J. Chem. Phys. **81**, 511 (1984).
[27] E. Ruckenstein and S. V. Gourisankar, J. Colloid Interface Sci. **107**, 488 (1985).
[28] A. Ulman, S. D. Evans, Y. Shnidman, R. Sharma, J. E. Eilers, and J. C. Chang, J. Am. Chem. Soc. **113**, 1499 (1991).
[29] B. Michel, H. Rohrer, L. Häussling, and H. Ringsdorf, Angew. Chem. Int. Ed. Engl. **30**, 569 (1991).
[30] C. A. Widrig, C. A. Alves, and M. D. Porter, J. Am. Chem. Soc. **113**, 2805 (1991).
[31] K. A. Motakabbir and M. L. Berkowitz, Chem. Phys. Lett. **176**, 61 (1991).
[32] J. Penfold and R. K. Thomas, J. Phys. Condens. Matter **2**, 1369 (1990).

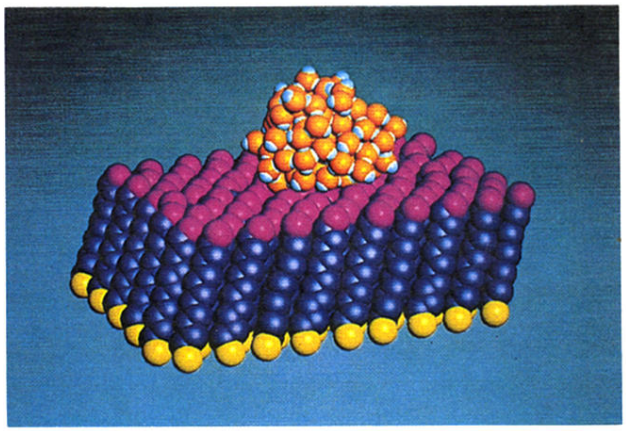

FIG. 1. Final configuration from a simulation of water molecules on a methyl-terminated monolayer. The molecules making up the layer consist of a sulfur headgroup (yellow), CH_2 pseudoatoms (blue), and a methyl tailgroup (purple). The O atom on the water molecule is orange and the H is white.

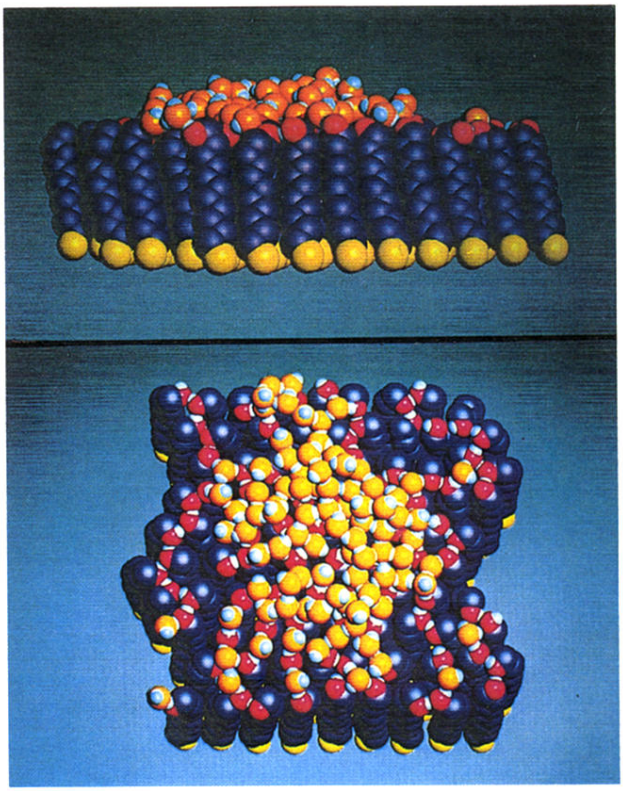

FIG. 3. Two views of the final configuration for water molecules on a monolayer with polar (-OH) tailgroups. The colors are as in Fig. 1 with the addition of O (red) and H (white) tailgroup atoms.

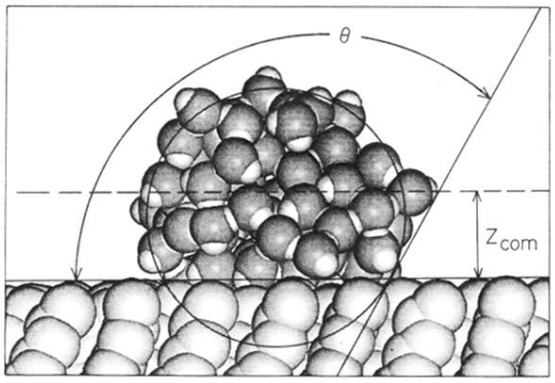

FIG. 4. Construction used to calculate a microscopic contact angle from time-averaged water configurations, superimposed on a view of the configuration shown in Fig. 1.